UNIVERSITY OF PITESTI
FACULTY OF MECHANICS AND TECHNOLOGY

SCIENTIFIC BULLETIN
AUTOMOTIVE series, year XV, no.19, vol. A

MICROSTRUCTURE-TRANSPORT PROPERTY RELATION IN YTTRIA- DOPED ZIRCONIA A MATERIAL USE TO CONTROL ENGINE COMBUSTION

Alin Rizea[1], Marioara Abrudeanu[1], Georgette Petot-Ervas[2], Claude Petot[2]
[1]University of Pitesti, Romania
[2]Ecole Centrale Paris, France

Abstract *Transmission electron microscopy, XPS analysis, electrical conductivity and diffusion measurements have allowed us to show the microstructure-transport property relation in ZrO_2- 9.0 mol% Y_2O_3 (YSZ) and Al_2O_3–YSZ composites. Samples with no detectable amorphous grain boundary precipitates show the highest grain boundary electrical conductivity (σ_{gb}) and oxygen diffusion coefficient (D_O) values, which decrease in presence of alumina additions. On the contrary, alumina additions (≤ 2 mol%) lead to an increase of the transport properties of samples showing grain boundary glassy films. These results were attributed to a decrease of the grain boundary wettability by the glassy phase when the alumina amount increases. Furthermore, the same grain boundary activation energy found for the different samples show that only ″clean″ grain boundaries contribute to the transport processes*

Keywords: Yttria - stabilized zirconia, electrochemical measurements, electrical conductivity

INTRODUCTION

Yttria-stabilized zirconia (YSZ) is by far the main solid electrolyte in electrochemical devices and it is still one of the prime candidates for use in oxygen gauges to control engine combustion, for instance. This material is presently employed at temperatures above 600°C. However, for cost reduction and long term stability it is always a demand to reduce the operating temperature of the devices.
In this study microstructural and nanochemical features of yttria-stabilized zirconia (YSZ) and Al_2O_3–YSZ composites were investigated in order to understand their influence on the ionic conductivity and oxygen diffusion of this solid electrolyte.

EXPERIMENTAL

The different samples were sintered either from 9.0 mol % Y_2O_3 doped-zirconia powders prepared by the freeze-drying method (samples Z_F) or from 9.9 mol% Y_2O_3 doped-zirconia powders supplied by Rhone Poulenc (samples Z_C) [1,2]. These powders were isostatically pressed at 2000 bar or 4000 bar. They are sintered at different temperatures between 1250 ° and 1600 °C. The main impurity is silicon. Samples Z_C are less contaminated (~0.42 wt % $Si0_2$) while samples Z_F contain: ~1.0 wt % $Si0_2$. The composites Z_C were prepared by mixing in alcohol the powders during several hours. The composites Z_F were prepared by adding $Al_2(SO_4)_3$ (99.99wt %) to the precursor used to prepare samples Z_F (water solution of zirconium and yttrium sulphates)
The electrical conductivity was characterized by complex impedance spectroscopy [1, 2], using silver as electrode material.

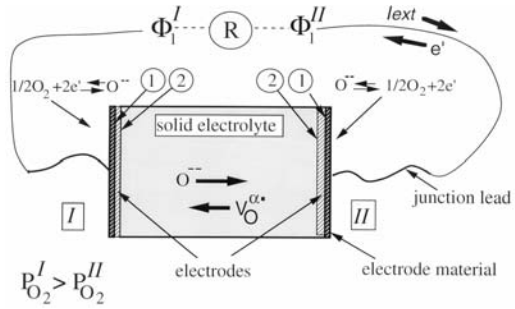

Fig. 1. Experimental arrangement for electrochemical measurements (E_{open}, t_{ion}, D_O)

The ionic transference number (t_{ion} ($=\sigma_{ion}/(\sigma_{ion}+\sigma_{el})$) and oxygen diffusion coefficient (D_O) were determined by the electrochemical method [3, 4]. One can recall that the principle of the method is to place the opposite sides of the sample (Fig. 1), coated with the same electrode material, between reversible electrodes (oxide / electrode material interfaces) subjected to different oxygen partial pressures.

In open circuit conditions (Fig. 1- $I_{ext} \approx 0$), the terminals of the cell are connected to a high impedance millivoltmeter ($R > 10^{13}\Omega$). The interfacial reactions ($O^{--} <=> 1/2O_2 + 2e'$) are then controlled by the electron transfer in the oxide. In presence of the same electrode material, the chemical potential of the electrons is the same at the cell terminals à) and the cell generates an open circuit voltage given by:

$$E_{open} = \Phi_1^I - \Phi_1^{II} = t_{ion}\,\frac{RT}{4F}\ln\frac{P_{O2}^I}{P_{O2}^{II}} \qquad (1)$$

where ($\Phi_1^I - \Phi_1^{II}$) is the electrical potential difference measured at the cell terminals and P_{O2}^I and P_{O2}^{II} the oxygen partial pressures in equilibrium with sides I and II of the oxide, respectively.

In short circuit conditions (Fig1- R=0, Iext≈I_{SC}), the terminals of the cell are at the same electrical potential ($\Phi_1^{II} = \Phi_1^I$). In presence of the same electrode material ($(\eta_e)_1^{II} = (\eta_e)_1^I$) the leakage current in the solid electrolyte is zero and the interfacial reactions ($O^{--}<=>1/2O_2+2e'$) take place due to the electron transfer, via the external circuit. Consequently, the ionic flux $J_{O^{--}}$ through the compound is proportional to the current density (i_{sc}) in the external circuit ($i_{sc} \approx -2F\,J_{O^{--}}$). If one neglects the correlation effects, the diffusion coefficient of the oxygen ions is given by:

$$D_O = g\,\frac{RT}{4F^2 C_{O^{--}}}\,\frac{I_{SC}}{E_{open}} \qquad (2)$$

with g=L/s, I_{sc}=s i_{sc} and where "s" is the area of the electrode surface, L the oxide thickness, $C_{O^{--}}$ the concentration of oxygen ions per cm^3 and E_{open} the open circuit voltage (Eq.1).

The short-circuit current (I_{sc}) is obtained by extrapoling the data U = f(I) to U = O, where U is the voltage determined at a variable resistance R placed in the external circuit (Fig. 1). Silver was used as the electrode material because it allows to satisfy the reversible electrode conditions [3, 4]. Furthermore, the ratio P_{O2}^I / P_{O2}^{II} is chosen close to one to satisfy the ideal conditions to determine D_O.

EXPERIMENTAL RESULTS

MICROSTRUCTURAL CHARACTERIZATION AND NANOCHEMICAL ANALYSIS

The TEM and SEM observations show that samples Z_C sintered at 1350 °C present a poor microstructure. All the triple points are glassy with a continuous glassy film at grain boundaries

immediately adjacent (Fig. 2). Samples Z_F, sintered in the same conditions, show a cleaner microstructure. Only a fraction of triple points (~1/5) shows lenticular glassy precipitates which do not wet the adjacent grain boundaries (Fig. 2). The microstructure is cleaner when sintering is performed at higher temperatures. However, the cleanest microstructures are observed for samples Z_F sintered at 1600°C, for annealing times t ≥30 h (Fig. 3a). The grain size is then close to 20 μm and the lenticular precipitates are present at all triple points, with spherical glass pockets widely dispersed in the grains. TEM and SEM characterizations show that the microstructure is not greatly influenced by alumina additions ≤ 5 mol%. Small alumina aggregates were occasionally observed in some grain boundaries of the composites Z_F (Fig. 3b), while a higher density of larger aggregates of this secondary phase was observed in composites Z_C.

Table 1. TEM X-ray microanalysis results in wt % in amorphous precipitates

samples	Triple points			Glass pokets	
	Al	Si	Al/Si	Al	Al/Si
Z_C / 1350 °C - 5 h	~ 4.0	~20	~1/5	~28	~5/1
Z_F / 1600 °C - 5 h	~25	~26	~1/1	~25	~1/1
Z_F / 1600 °C - 40 h	~10	~41	~1/4	~36	~3/1

EDAX analysis shows that the main impurities are Al and Si. Their intragranular amount is nearly the same for the different materials (Al ~ 0.1wt %, Si ~ 0.5 wt %). These impurities are mainly concentrated in the grain boundaries glassy phases and in the glass pockets dispersed in the grains (Table 1). In the samples without alumina, the amount of Al is generally higher than that of Si in the glass pockets dispersed in the grains. In the grain boundaries, the results reported in Table 1 indicated only a tendency (size of the glassy phases comparable to the size of the available probes). However, it seems that the amount of Si is higher than that of Al. Furthermore, the glass phases in the Z_F materials contains generally higher concentrations of Al and Si and therefore smaller amounts of Zr and Y. On the other hand, the differences in composition between samples Z_F treated at 1600 °C for 5 and 40 h, indicates that impurities redistribution occurs as the glass is concentrated in fewer and fewer pockets when the grain size increases. For the composites, the amount of Al was found always higher than that of Si with an average Al/Si ratio close to ~30 (mean value of Al ~60 wt% in the triple points and ~30 wt % in the glassy pockets).

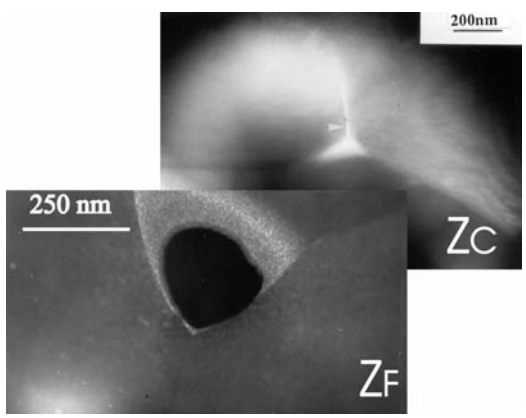

Fig. 2. Grain boundary microstructure of the Z_F and Z_C samples.

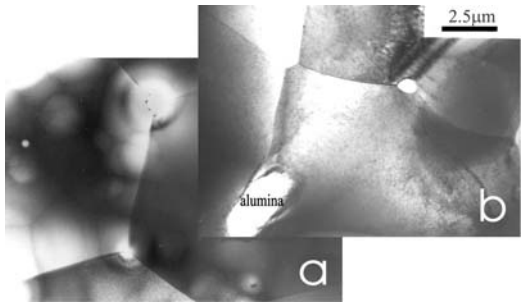

Fig. 3. Grain boundary microstructure of the Z_F sample (a) sintered at 1600 °C, for 40 h, and of the Z_F composite (b) sintered at 1350 °C, for 5 h.

On the other hand, XPS analysis, performed on the fracture surface of YSZ samples have shown that cation redistributions occur during cooling [5]. In the first monolayers at the periphery of the grains we have found that the amount of Si is nearly the same in the different samples, while the depth profile (depth close to 600 nm) decreases more rapidly in the slowly cooled sample than that in the quenched material. These results suggest that a higher amount of Si was rejected from grains to grain-boundaries in the slowly cooled sample, leading to the formation of SiO_2 precipitates. This higher amount of glassy phase at grain boundaries has allowed us to explain the lower values of σ_{gb} found for the slowly cooled sample.

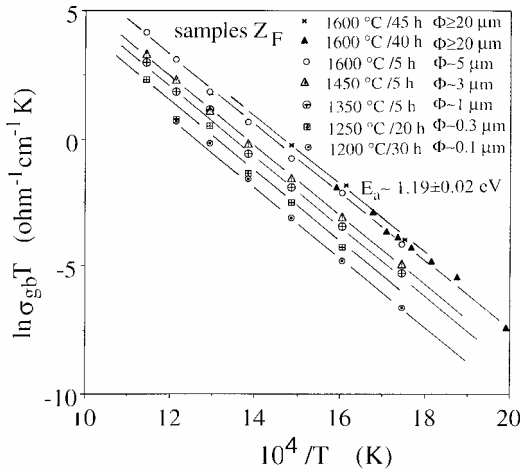

Fig. 4. Influence of the grain size on the grain boundary conductivity of samples Z_F

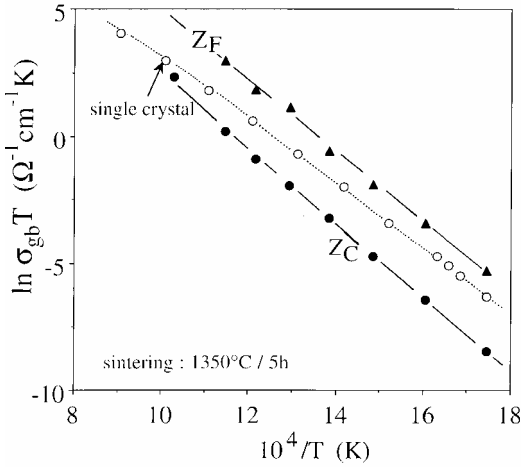

Fig. 5. Grain boundary conductivities of samples Z_C and Z_F. Comparison with the bulk conductivity of a single crystal (YSZ - 9 mol% Y_2O_3)

INFLUENCE OF THE STARTING MATERIALS ON THE BULK AND GRAIN BOUNDARY CONDUCTIVITIES

In order to prevent kinetic demixing effects all the following results have been obtained with sample cooled at the furnace cooling rate, at the end of sintering. As in previous works [1 - 4], we have found that the bulk conductivity (σ_b) values are close to those of a single crystal and that the grain boundary conductivity (σ_{gb}) increases with the sintering temperature, as illustrated Fig. 4 for samples Z_F. Furthermore, we have found that the grain boundary conductivity of samples Z_F ($Si0_2$ ~1.0 wt %) is higher than that of samples Z_C, less contaminated with silica ($Si0_2$ ~0.42 wt %) (Fig. 5). This apparent discrepancy shows the key role played by the location of the grain boundary glassy phase, as we shall see later.

BULK AND GRAIN BOUNDARY CONDUCTIVITIES OF YSZ ALUMINA COMPOSITES

Fig. 6 shows that the grain-boundary conductivity of samples Z_F (~1.0 wt % $Si0_2$) decreases in presence of alumina additions, while samples Z_c, less contaminated with silicon (~0.43 wt % $Si0_2$), show a maximum of σ_{gb} near 2 mol % Al_2O_3 when sintering occurs at 1350 °C or near 1 mole % Al_2O_3 when it was performed at 1600 °C.

OXYGEN DIFFUSION COEFFICIENT

The experiments have been performed with oxygen and air flowing in compartments I and II, respectively (Fig. 1).

Fig. 7 shows that the values of D_O obtained (Eq.2) with samples Z_F sintered at 1600 °C, for 40 h, are in good agreement with those of an yttria (9.5 mole %)-doped zirconia single crystal [4, 7]. The diffusion entities and jump frequencies involved in these two samples are then very close. In Fig. 7, we also reported the conductivity diffusion coefficient ($D\sigma$) calculated from the conductivity values (σ_i), using the Nernst - Einstein relation and assuming that the correlation factor (f_i) of the generalized form [8] is equal to one :

$$D_{\square} = f_i \frac{\sigma_i kT}{(z_i e)^2 C_i} \qquad (3)$$

where C_i is the number of oxygen ions per cm^3 and k the Boltzmann constant.

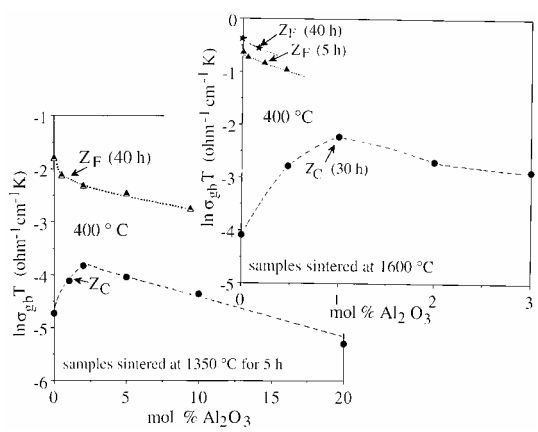

Fig. 6. Influence of the amount of alumina on σ_{gb} of samples Z_C and Z_F

Remark. As shown by Kikuchi and Saito [8], the correlation factor g has a similar meaning as the correlation factor for the tracer diffusion. It is equal to one when all the sites are equivalent (isolated defects).

Fig. 7 shows also that $D_O < D\sigma$. This difference indicates both that in presence of an applied electrical field all the sites involved in the transport processes are not equivalent and that they are different of those involved in diffusion (i.e. when the driving force is due to the concentration gradient). These results are then consistent with the presence of complex defects, in the experimental range investigated.

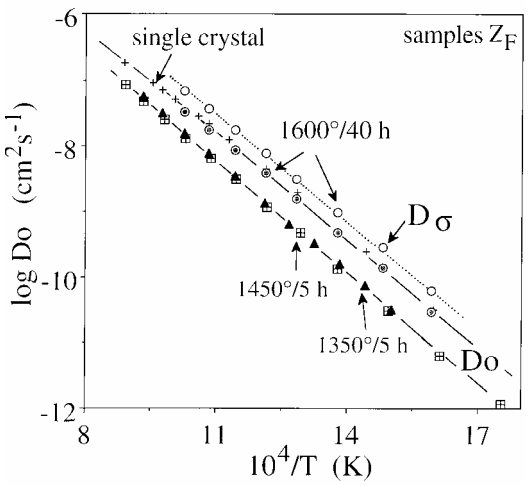

Fig. 7. Oxygen diffusion coefficient of sample Z_F sintered at 1600 °C for 40 h. Comparison with the values obtained with a single crystal [7] and with those of $\tilde{D}_\sigma$

CONCLUDING REMARKS

The set of results obtained in this work shows the influence of the grain boundary wettability by the glassy precipitates on the transport processes. The higher grain boundary conductivity values of samples Z_F ($Si0_2$ ~1.0 wt %, Al_20_3 ~10 wt ppm) seem to be due to the microstructure of the grain boundaries which are free of detectable glassy phases and show lens shape amorphous precipitates at triple points (Fig. 2). On the contrary, samples Z_c less contaminated with Si and Al ($Si0_2$ ~1.0 wt %, Al_20_3 <10 wt %), show a high density of wetted grain boundaries (Fig. 2) and small alumina additions (≤ 2mol%) lead to an increase of σ_{gb} (Fig. 6). According to the microchemical analysis (Table. 1), these results can be explained by the composition of the glassy phases. The lower wettability of grain boundaries of the Z_F samples seems to be due to their higher amount of Al and Si (Table 1). This assumption is consistent with the results obtained with the composites. In presence of alumina additions (Al/Si~30 compared to Al/Si ≤1, Table. 1), the higher amount of Al (Al~60 wt %) found in the glassy phases leads likely to an increase of its viscosity and a partial dewetting of the grain boundaries. When the amount of alumina in samples Z_C increases (Fig. 4), σ_{gb} reaches a maximum (around 2 mol% or 1 mol % when sintering occurs at 1350 °C or at 1600 °C, respectively). It appears then a competitive effect between the beneficial influence of alumina on the glassy phase viscosity and the isolating behaviour of the alumina particles not dissolved in the siliceous precipitates. In agreement with these conclusions, alumina addition to the polycrystals Z_F, lead to a decrease of the intergranular conductivity (Fig. 6), due to the prevailing influence of the insulating behaviour of the alumina particles largely dispersed in the material (Fig. 10). It should be noted that the previous analysis is consistent with the conclusions of Badwall et al. [9], when they assume that alumina acts as a "scavenger" for SiO_2.

Furthermore, we have found the same activation energy of the grain boundary conductivity for the different materials, in spite of significant differences of microstructure. This result is in agreement with intergranular conduction processes taking place only through ″clean″ grain boundaries.

REFERENCES

1- Filal M., Petot C., Mokchah M., Chateau C., Charpentier J.L., Sol.St.Ionics, 80, 27-35 (1995)
2- Petot C., Filal M., Rizea A., Westmacott K., Laval J.Y., Lacour C., J.Eur.Cer.Soc., 18,1419-1428 (1998)
3-.Petot-Ervas G., Rizea A., Petot C. , Ionics 3, 405- 411 (1997)
4- Petot-Ervas G., Petot C., Solid .State Ionics, 117, 27-39 (1999)
5- Rizea A., Chirlesan D., Petot C., Petot-Ervas G., Solid State Ionics, 146, 341-353 (2002)
6- Badwal S.P.S., Solid State Ionics, 76, 67 (1995)
7 Solmon H., Chaumont J., Dolin C., Monty C., Cer. Transactions, Amer. Cer. Soc. 24, 175 (1992)
8- Sato H., Kikuchi R., J. Chem. Phys. 55 (2) 677-702 (1971)
9- Badwall S.P.S., Drennan J., Sol. Stat. Ionics, 40:41, 869-873 (1990)